Available online at www.sciencedirect.com
ScienceDirect
Journal of Power Sources 174 (2007) 41–48
JOURNAL OF POWER SOURCES
www.elsevier.com/locate/jpowsour

Spiral wound valve-regulated lead-acid batteries for hybrid vehicles

M.L. Soria*, F. Trinidad, J.M. Lacadena, J. Valenciano, G. Arce

Exide Technologies, Research & Development Centre, Autovía A-2, km 42, E-19200 Azuqueca de Henares, Spain

Received 29 December 2006; received in revised form 9 April 2007; accepted 10 April 2007
Available online 24 April 2007

Abstract

Future vehicle applications require the development of reliable and long life batteries operating under high-rate partial-state-of-charge (HRPSoC) working conditions. This paper updates work carried out to develop spiral wound valve-regulated lead-acid (VRLA) batteries for vehicles with different hybridisation degrees, ranging from stop-start to mild hybrid applications.

Former work on design optimisation and active material formulations has been implemented in two spiral wound VRLA batteries, rated 12 V 50 Ah and 6 V 24 Ah, and these two products are currently being tested both in benches and in vehicles with different hybridisation degrees within a demonstration project funded by the Advanced Lead Acid Battery Consortium and in collaboration with several European vehicle and electrical component manufacturers.

Keywords: Valve-regulated lead-acid batteries; Spiral wound; Stop-start; Microhybrid, mild hybrid vehicles

1. Introduction

The already announced legislations on the reduction of vehicles emissions and fuel consumption levels have led in past years to the development of vehicles with different powertrain hybridisation degrees, implementing new functions, such as engine stop-start operation, regenerative braking, and different levels of hybrid electric propulsion assist [1]. Depending on the power requirements and vehicle hybridisation degree, several drivetrain and powernet architectures, with nominal voltages ranging from 14 V to nearly 300 V in automobiles and over 600 V in hybrid buses, have been proposed [2].

According to the EUCAR Well-to-Wheels Report [3], hybrid vehicles can provide, by 2010, an additional energy reduction of about 15–18% to the results obtained from further developments in energy efficiency and vehicle technology, thus contributing to CO_2 emissions reductions (Kyoto protocol) through reduced fuel consumption. Hybrid vehicles, either with conventional internal combustion engines in the short-medium term, or with a fuel cell as energy generation device, need a battery to store energy generated during cruising periods and regenerative braking. This energy would then be required for vehicle starting and acceleration (booster), besides keeping all consumers working during vehicle stops.

No battery system alone represents up to date a solution, in terms of energy/power performance, life and cost goals, industrial development and recycling facilities, to cope with the stringent performance and cost demands of car manufacturers [4]. Different electrochemical systems have been installed either in commercial hybrid vehicles or in demonstration prototypes: high voltage Ni-MH batteries in the well known hybrid vehicles Toyota Prius, Honda Insight or Ford Escape, a valve-regulated lead-acid (VRLA) 12 V battery in the Citröen C3 with stop-start function and a Li-ion 346 V battery in the Nissan Tino [5].

Efficient energy management in vehicles with such functions demands the development of batteries with improved charge acceptance as well as longer life under high-rate partial-state-of-charge (HRPSoC) working conditions. Specific demands of each hybridisation degree, as well as cost considerations, have allowed to establish which battery types, already in the market or under development, fit better to the performance requested [1].

Lead-acid batteries are nowadays extensively used in automotive applications for engine starting, lightning and ignition

* Corresponding author. Tel.: +34 949 263 316; fax: +34 949 262 560.
E-mail addresses: MariaLuisa.SORIA@eu.exide.com (M.L. Soria), Francisco.TRINIDAD@eu.exide.com (F. Trinidad), JoseManuel.LACADENA@eu.exide.com (J.M. Lacadena), Jesus.VALENCIANO@eu.exide.com (J. Valenciano).

0378-7753/$ – see front matter © 2007 Elsevier B.V. All rights reserved.
doi:10.1016/j.jpowsour.2007.04.035

(SLI) [6]. However, advanced vehicle requirements demand battery working regimes mainly under partial-state-of-charge (PSoC) conditions, that, in the case of flooded batteries, lead to premature capacity loss provoked by electrolyte stratification [7] and active material irreversible sulphation [8]. Changes in the demands on automotive batteries [9] are caused by the increase of on-board power requirements due to the introduction of new features in the vehicles to provide enhanced safety and comfort, such us the replacement of mechanical by electrical functions (steer- and brake-by-wire, air conditioning,. . .), as well as of novel functions (stop-start, regenerative braking, etc.) aimed at achieving significant fuel consumption and emission savings.

The increase of electric functions in the vehicles has provoked an evolution of conventional flooded batteries in order to enhance power capability (thinner plates with improved corrosion resistant alloys for the grids [10]), to improve life under deep cycle conditions and to reduce water consumption along life.

Valve-regulated lead-acid (VRLA) batteries are also available for vehicles which demand high power linked to a higher capacity throughput due to the higher vehicle energy consumption demands [11]. Moreover, VRLA batteries with spiral wound design provide outstanding performance in terms of power capability and life under different cycling conditions when compared to prismatic designs [12].

VRLA batteries are today the most cost effective solution for short term low voltage applications (14–42 V powernets), due to their availability, cost and low temperature performance. AGM technology is commonly used, due to the high power capability demanded, the improved life when compared with flooded designs, and its intrinsic maintenance free characteristics, as well. However, main drawbacks of VRLA batteries when compared to Ni-MH batteries are their limited charge acceptance and capacity turnover over the battery life under partial-state-of-charge (PSoC) working conditions and their reliability under real operation conditions [13].

2. Experimental

2.1. Battery assembly

The development of batteries for hybrid vehicles was based on the outstanding power and life characteristics of Orbital™ spiral wound VRLA batteries, which present the following main design features [12]:

- High purity lead-tin grids, with higher corrosion resistance.
- Active material formulations adapted to the battery working conditions.
- Absorbent glass mat separators that optimise recombination process and prevent premature paste shedding, and with an specific formulation to reduce electrolyte stratification whereas mechanical properties are adapted to the assembly process conditions.

Table 1
Characteristics of Orbital™ VRLA batteries for HEV applications

Dimensions/$L \times W \times H$ (mm)	$260 \times 173 \times 206$	$65 \times 175 \times 190$
Weight (kg)	18.0	4.7
Nominal voltage (V)	12	6
Nominal capacity, C_{20} (Ah)	50	24
Cold cranking (A) (−18 °C, EN 50342)	800	400

- Multiple pressure release valves, one per cell, and isolated cell design that provide higher battery safety and durability.
- Through-the-partition intercell welds, with lower internal resistance and higher reliability.
- Cooling channels that allow for an efficient battery thermal management by means of air draught cooling systems, thus increasing operating life in warm environments.

Product development was focused on two different battery sizes, to comply with the requirements of the car manufacturers for micro- and mild hybrid vehicles: a 12 V 50 Ah battery for vehicles with stop-start function, both conventional and micro-hybrids with 14 V powernet and also for hybrid buses, and a 6 V 24 Ah module for mild hybrid vehicles, mainly with medium powernet voltage (42–60 V) [14]. This 6 V module can provide attractive packaging solutions for vehicles with 18, 24, 30, 36, 48 or 60 V battery nominal voltages. The dimensions and nominal electrical characteristics of both battery types are indicated in Table 1.

Previous work on active material formulations showed that addition of 1.5% expanded graphite, characterised by high specific surface area, to the negative active material formulation proved to be very effective to avoid sulphation under high-rate PSoC conditions [15], linked to adequate rheological characteristics of the active material during the plate manufacturing processes. Moreover, the formulation of positive active material was also optimised to provide the best compromise between power capability and life performance.

Finally, according to previous studies on valve opening pressure and electrolyte saturation degree [16], manufacturing process conditions were adjusted to assure a high initial saturation degree that might suppress any eventual negative active material oxidation. Moreover, the increased electrolyte reserve could also be beneficial for high temperature applications and with difficult charge control.

Two types of graphite compounds have been tested in the negative active material formulations of 6 V 24 Ah modules. They have been referenced G-1 and G-2 and, although manufacturing conditions were different, they showed equivalent BET specific surface area and average particle size values ($24\,m^2\,g^{-1}$ and 9.8 μm, respectively, for G-1 and $20\,m^2\,g^{-1}$ and 8 μm, respectively, for G-2).

2.2. Electrical testing

Electrical testing of the batteries was carried out with computer controlled cycling equipment: Bitrode LCN-7-100-12 for initial characterisation and cycle life tests of the batteries,

Digatron UBT BTS-500 mod. HEW 2000-6BTS in high-rate discharges and Digatron HEW 2000/12-700/36 BTS-600 for peak power/charge acceptance tests.

Preliminary characterisation of the batteries included capacity at 20 h rate (25 °C), reserve capacity (25 A, 25 °C) and cold cranking at −18 °C according to EN 50342 standard (10 s discharge at the rated cold cranking current +10 s rest + discharge at 0.6 times the rated cold cranking current to 1.0 V cell^{-1} as cut-off voltage). The recharges were also carried out according to EN 50342 standard (20 h/0.25 C A/2.4 V cell^{-1} + 4 h/0.025 C A, being C the nominal capacity at the 20 h rate).

A specific testing procedure was defined to calculate peak power on discharge and charge acceptance of the batteries at different states of charge (SoC). In the testing sequence, the batteries were tested at 100, 80, 60, 40 and 20% SoC and discharged during 10 s at 1.66 V cell^{-1} and charged during 5 s at 2.67 V cell^{-1} at the rated currents defined for each battery size. Moreover, ac internal resistance (Milliohmeter Hewlett Packard model 4338-B at 1 kHz and 25 °C) and open circuit voltage (OCV) were also measured at each SoC level.

The batteries have been tested according to three different cycle life profiles, depending on the envisaged applications.

2.2.1. Stop-start profile

This profile includes first a discharge period at a moderate current that takes into account the standard consumptions of the vehicle. These consumptions are simulated by a discharge at the 1 C rate approximately. However, simulation of vehicle starting by means of a short duration (1 s) high current discharge (300–400 A) is only considered by some car manufacturers, whereas others adjust the duration of the moderate discharge period to the estimated cycle DoD. In order to simplify the testing profile, cycling of 50 Ah batteries is carried out at 50 A (1 C rate). Before each life unit, the batteries are discharged 20% of their nominal capacity, in order to reach the 80% SoC level, whereas the 50 A/72 s discharge represents 2% DoD in each cycle. The duration of recharge at 50 A/14.4 V has been adjusted to recover the previously discharged capacity and thus maintain SoC level along the cycling test.

The starting capability of the battery is simulated by performing, at the end of each series of 20,000 cycles, two consecutive 3 s discharges at ambient temperature, at 500 and 250 A, that simulate starting of diesel and gasoline engines, respectively.

After each life unit, capacity and cold cranking at −18 °C are checked, as well as battery weight and ac internal resistance, to follow the evolution of these parameters along the battery life. The life test continues till one of the following failure criteria is reached:

- $V < 7.2$ V during the 500 and 250 A 3 s discharges.
- $V < 10.5$ V during cycling.
- Control capacity $< 0.5 C_{20}$.

2.2.2. Shallow PSoC cycling at 17.5% DoD

Performance of the batteries according to moderate rate PSoC cycling conditions has also been checked at 50% SoC, with *C*/3 rate charges and discharges at 17.5% DoD. Every 85 cycles the batteries were fully recharged to check available capacity, weight and ac internal resistance. The failure mode criterion was when the battery reached 10.0 V during any of the discharge steps.

2.2.3. Power assist profile

Finally, the third life test selected corresponds to EUCAR power assist profile: cycling at 60% SoC and 2.5% DoD with discharges at 5 C rate and charge steps at 4.5, 2 and 1 C rates [17]. This profile simulates vehicle boost during acceleration and recovery of braking energy in 120 s cycles. During the test, the batteries were air draught cooled by means of fans located under the modules. Every 10,000 cycles the C_2 capacity, ac internal resistance and weight loss of the batteries were checked. Battery failure criteria were capacity under 50% and voltage lower than 1.5 V cell^{-1} during cycling. Charge voltage was limited (<2.5 V cell^{-1}) in order to reduce overcharge and water loss.

When the batteries reached the respective failure criteria for each life test, they were recharged and torn down to determine the failure mode. Chemical analyses of the active material samples were carried out using internal volumetric (PbO_2) and gravimetric ($PbSO_4$) procedures. Active material porosity was measured with a mercury intrusion porosimeter Micromeritics Autopore 9405 and specific surface (BET) with a Micromeritics FlowSorb II 2300.

3. Results and discussion

3.1. Initial characterisation of 12 V batteries and 6 V modules

Table 2 shows the results of the preliminary characterisation according to EN 50342 of the batteries and modules, as well as the testing conditions in each case. Moreover, Fig. 1 shows the open circuit voltage, similar for both battery sizes when represented in V cell^{-1}, and the ac internal resistance for 12 V batteries and 6 V modules, at different states of charge ranging from 100 to 20% SoC. Internal resistance, which is indicated as percentage of the internal resistance value at 100% SoC, increases around 30% when the batteries are discharged to 20% SoC.

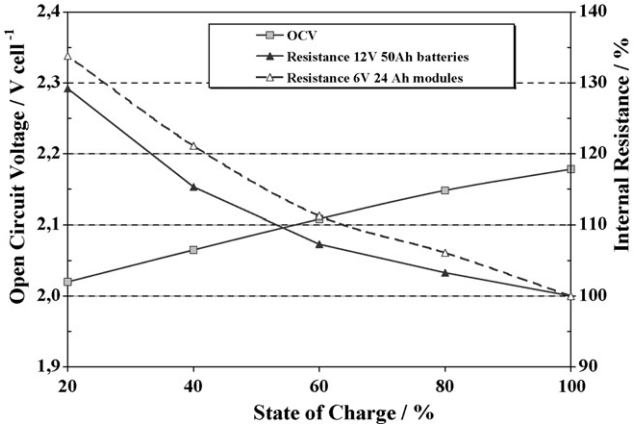

Fig. 1. Voltage and internal resistance vs. state of charge of Orbital^{TM} HEV 12 V/50 Ah batteries and 6 V/24 Ah modules.

Table 2
Initial electrical test results of 12 V/50 Ah batteries and 6 V/24 Ah modules

Reference	Resistance (mΩ)	Capacity		Reserve capacity (min)	Cold cranking EN 50342		
		I (A)	C_{20} (Ah)		I (A)	$V_{10\,s}$ (V)	Duration (s)[a]
12 V/50 Ah	2.61	2.50	52.3	110	800	8.29	83
6 V/24 Ah	2.24	1.20	24.4	42.3	400	4.28	100

[a] Duration to 1.0 V cell^{-1} calculated according to EN 50342.

3.2. Power capability characterisation

Fig. 2 shows the 10 s average power on discharge and 5 s average charge acceptance at 2.67 V cell^{-1} of 12 V 50 Ah batteries and 6 V 24 Ah modules, both expressed as W kg^{-1}. Discharge power was measured at 800 A/10.0 V for 12 V batteries and 400 A/5 V for 6 V modules. Charge acceptance test was carried out at 2.67 V cell^{-1} in both cases, although it was limited for 12 V batteries at SoC $\leq$ 40% by the maximum current output of the testing equipment (390 A). 10 s peak power outputs of 7 and 2 kW can be obtained, at 100% SoC, from each 12 V 50 Ah battery and 6 V 24 Ah module, respectively, equivalent to 380–420 W kg^{-1}. At 60–80% SoC, which is considered the optimised battery working conditions in hybrid vehicle operation, average 10 s discharge power and 5 s charge acceptance values are around 350 and 130–150 W kg^{-1}, respectively.

3.3. Test of 12 V 50 Ah batteries according to stop-start cycle life profile

In order to compare the improved performance of HEV design and active material formulations when compared to standard SLI Orbital^{TM} batteries, three batteries of each type (HEV and SLI) were submitted to the stop-start cycling test described previously. Fig. 3 shows the capacity evolution along the test, as well as the EN cold cranking duration, measured after each life unit comprising 20,000 2% DoD microcycles (400 capacity turnover). Moreover, Figs. 4 and 5 show, respectively, the evolution of end of discharge voltage and the ac internal resistance measured, after a full recharge, at 25 °C and −18 °C for both

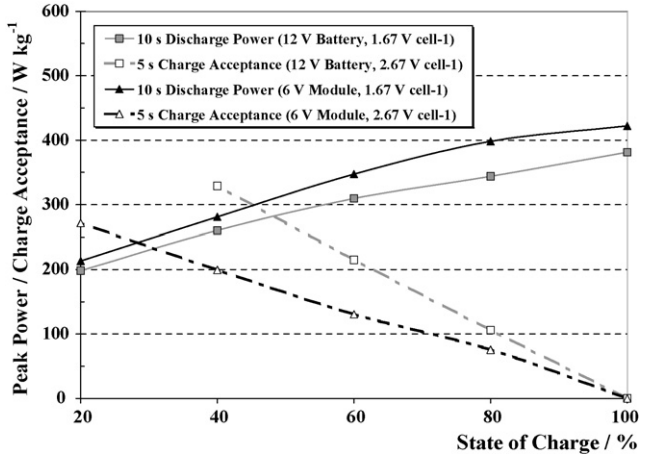

Fig. 2. Specific power and charge acceptance vs. state of charge of Orbital^{TM} HEV 12 V/50 Ah batteries and 6 V/24 Ah modules.

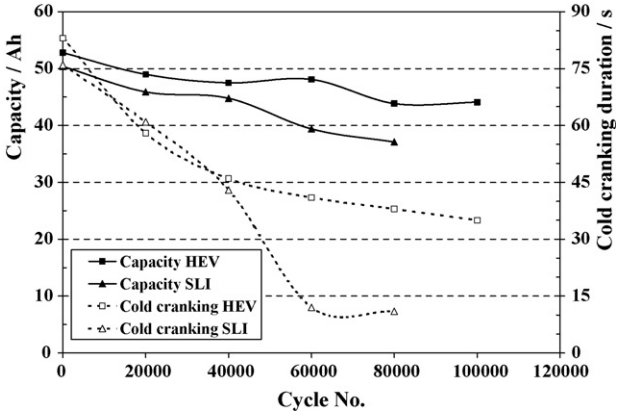

Fig. 3. Capacity and cold cranking duration evolution along stop-start cycle life test of 12 V/50 Ah batteries.

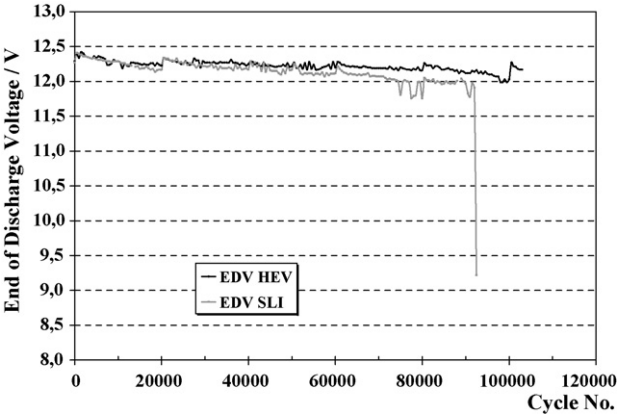

Fig. 4. End of discharge voltage evolution along stop-start cycle life test of 12 V/50 Ah batteries.

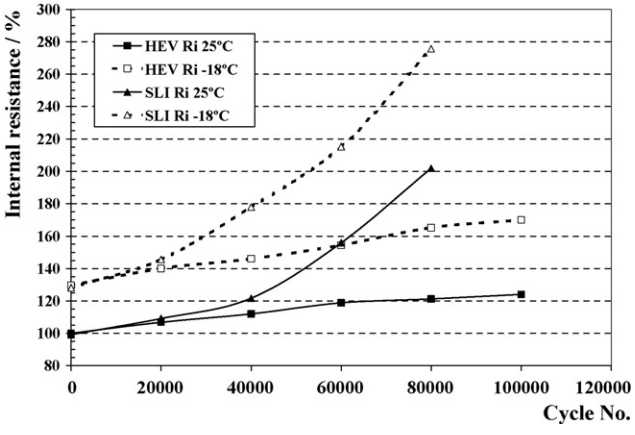

Fig. 5. Internal resistance evolution along stop-start cycle life test of 50 Ah batteries.

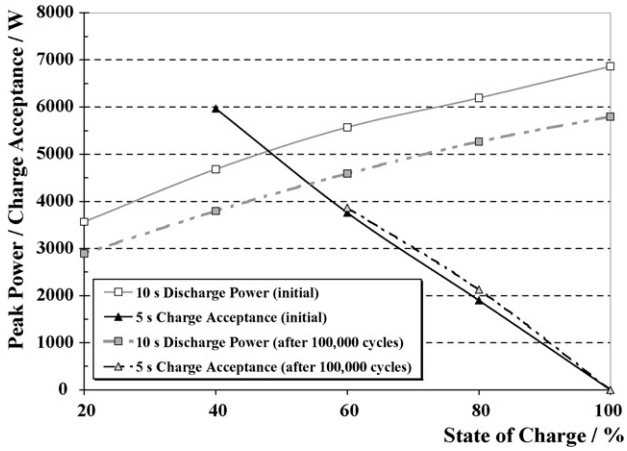

Fig. 6. Peak power and charge acceptance of Orbital^{TM} HEV 12 V/50 Ah batteries before aging test and after 100,000 stop-start cycles.

types of batteries. dc resistance values calculated from voltage drops during the 3 s discharges at 250 and 500 A at the end of each life unit, are slightly higher than the measured ac values due to polarisation phenomena.

SLI batteries failed after 80,000–90,000 cycles, whereas test of HEV batteries is still running. Results obtained up to date (110,000 cycles) show a more stable behaviour for HEV batteries in terms of capacity evolution, whereas the performance loss of SLI batteries, was mainly due to the sharp internal resistance increase, which was reflected in the end of discharge voltage evolution along the test and in the significant reduction of the cold cranking duration. Moreover, power capability characterisation of the HEV batteries after 100,000 cycles demonstrated that only 15–20% discharge power had been lost, as shown in Fig. 6, whereas charge acceptance is slightly better than the initial values.

3.4. Test of 6 V 24 Ah modules under PSoC conditions

Fig. 7 shows the capacity evolution of 6 V 24 Ah modules during the cycle life test at moderate rate and PSoC conditions (*C*/3 rate, 50–67.5% SoC, according to nominal capacity

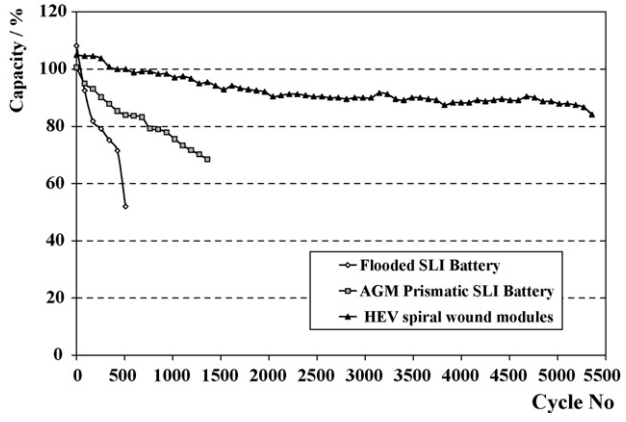

Fig. 7. Capacity evolution of lead-acid batteries along 17.5% DoD PSoC cycling.

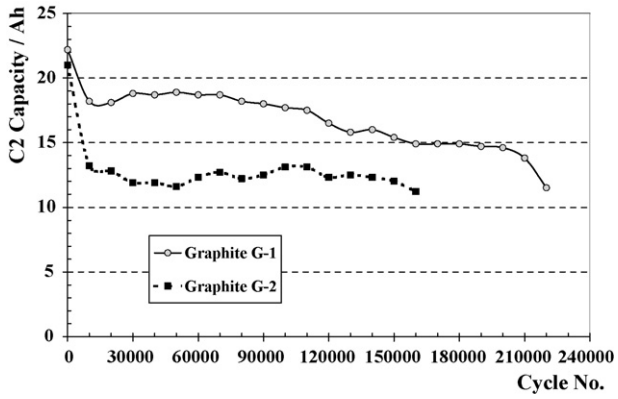

Fig. 8. Capacity evolution along power assist cycle life test (60% SoC, 2.5% DoD) of 6 V 24 Ah modules.

value), in comparison to SLI flooded and AGM VRLA batteries. The Orbital^{TM} HEV modules fulfilled 63 life units, i.e. over 5300 cycles or 930 times the nominal capacity, before reaching the voltage failure criterion ($V < 10.0$ V). This is an outstanding value, when compared to car manufacturers' requests for standard SLI flooded and AGM technologies (6 and 18 life units, respectively). Records of internal resistance evolution of the modules along the test, show that it increased 25% after around 3000 cycles, 50% after 4500 cycles and over 100% at the end of the life test.

3.5. Power assist cycle life test of 6 V 24 Ah modules

Fig. 8 shows the capacity evolution of 6 V 24 Ah modules with two different graphite types (referenced G-1 and G-2) in the negative active material formulation. There is a clear influence of the graphite characteristics both on the number of cycles completed before reaching the failure criterion (220,000 cycles for modules with graphite G-1 and 160,000 for those with graphite G-2) and specially on the capacity evolution along the life test. Capacity of modules with graphite G-1 is significantly better than that of modules with graphite G-2, probably due to better charge acceptance. As a consequence, sulphation is delayed in modules with graphite G-1 and thus internal resistance values along the life are lower, and this fact is reflected in the end of discharge voltage evolution along the test, as shown in Figs. 9 and 10.

3.6. Failure mode analysis

After reaching the failure criteria in the shallow PSoC and power assist life tests, the 6 V modules were torn down to establish the main ageing mechanisms. Tear-down analysis results are shown in Table 3, that includes three groups of modules tested: two groups with graphite G-1 in the negative active material formulation tested under moderate rate shallow PSoC and under power assist HRPSoC conditions and one group with graphite G-2 tested according to the power assist life profile. Analytical results of active materials from non-aged modules with graphite G-1 and G-2 have also been included for comparison purposes.

Table 3
Chemical composition, specific surface and porosity of negative and positive plates of 6 V 24 Ah VRLA modules, aged according to moderate and high rate PSoC conditions

Module batch and ageing conditions	Negative plates[a]		Positive plates			
	$PbSO_4$ (%)	BET ($m^2\ g^{-1}$)	PbO_2 (%)	$PbSO_4$ (%)	Porosity (%)	BET ($m^2\ g^{-1}$)
G-1 non-aged	4.7	0.72	86.3	5.9	47.8	5.7
G-1 5,355 cycles moderate rate[b]	2.1 (T); 15.0 (B)	0.58 (T); 0.60 (B)	93.2	2.1	58.8	1.75
G-1 217,000 power assist cycles[c]	39.3 (T); 10.4 (B)	0.51 (T); 0.69 (B)	95.1	1.3	55.6	0.90
G-2 non-aged	4.6	0.74	89.2	4.2	52.6	5.8
G-2 160,000 power assist cycles[c]	35.2 (T); 14.9 (B)	0.50 (T); 0.64 (B)	93.5	2.5	56.3	0.79

[a] T: top, upper part of the electrode; B: bottom, lower part of the electrode.
[b] 50% SoC, 17.5% DoD, *C*/3 rate.
[c] 60% SoC, 2.5% DoD, 5 C rate.

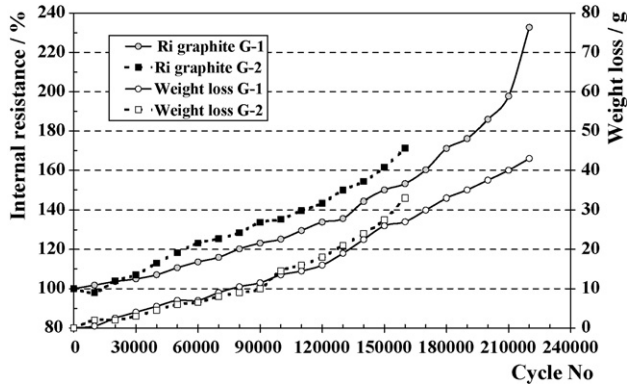

Fig. 9. Internal resistance and accumulated weight loss of 6 V 24 Ah modules along power assist cycle life test.

Results show significant differences in the ageing mechanisms of the two cycling profiles considered. Although the three groups of modules were tested under partial-state-of-charge conditions, the distribution of irreversible lead sulphate accumulated in the negative electrodes is rather different depending on the cycling rate and DoD. In the modules tested with moderate rate (*C*/3) charge/discharge conditions, lead sulphate is mainly in the lower part of the electrodes whereas in those tested according to the power assist high rate (up to 5 C) conditions, lead sulphate is predominantly located in the upper part of the electrodes.

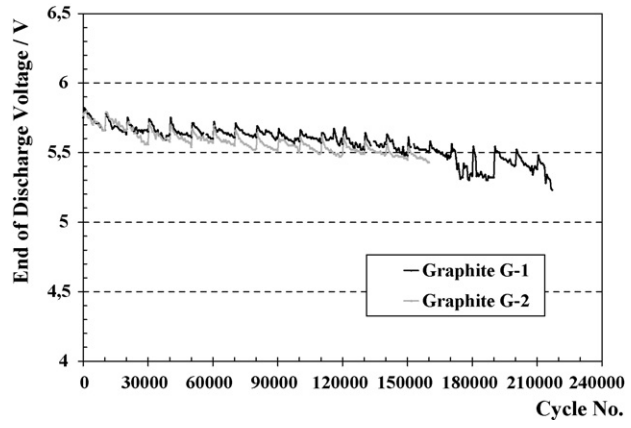

Fig. 10. End of discharge voltage evolution along power assist cycle life test (60% SoC, 2.5% DoD) of 6 V 24 Ah modules.

These results agree with previous studies with prismatic [18] and cylindrical AGM configurations. The mechanism explaining this failure mode of batteries tested according to high-rate PSoC profiles was proposed by Lam et al. [19]. Moreover, lead sulphate accumulation is accelerated by higher temperatures in the inner and upper part of the cells [15,16]. However, there are no significant differences between aged materials from modules tested according to the power assist profile and with graphite G-1 and G-2 in the negative active material formulations, therefore addition of graphite G-1 seems to delay the main ageing phenomenon, i.e. irreversible sulphation of the negative electrodes.

Concerning the positive active material, results show a higher porosity increase in modules tested according to moderate rate PSoC profile, a clear indication of active material degradation.

4. In vehicle tests

In order to validate the performance of HEV 12 V 50 Ah batteries and 6 V 24 Ah modules in real in-vehicle operating conditions, a demonstration programme started some months ago, involving different vehicles available commercially or as demonstrators [20].

4.1. Test of 12 V 50 Ah batteries in stop-start and microhybrid vehicles

PSA (FR) has provided two Citröen C3 Stop & Start vehicles, equipped with 1.3 L gas engine, semi-automatic gear box and starter generator (Fig. 11a). The vehicles are used as "conventional" cars, with daily use. Periodically, the batteries are removed from the cars and characterised in benches, to check weight, internal resistance, residual and real capacity and cold cranking.

Valeo (FR) is testing a 12 V/50 Ah battery in a Renault Clio (1.2 L; gasoline) with a stop-start system (first generation). As this vehicle is not equipped with a BMS (Battery Management System), this test is representative of severe working conditions. Tests are performed in urban, highway and hybrid circuits, recording vehicle speed and battery parameters (current, voltage, temperature in different battery positions).

Fig. 11. Micro- and mild hybrid vehicles for the demonstration programme: (a) Citröen C3 Stop & Start, (b) Ford Fiesta Microhybrid, (c) Mild hybrid VW Golf and (d) Mild hybrid Ford Transit van.

Another 12 V 50 Ah battery was installed by Ford (DE) in a Microhybrid Fiesta (Fig. 11b), a small 1.4 L gasoline passenger car with five-speed manual transmission and 14 V belt driven integrated starter generator (B-ISG) for stop-start operation, regenerative braking and stall recovery. This vehicle reaches a fuel economy benefit on NEDC homologation cycle of 5–6%. City driving with intuitive Human Machine Interface (HMI), allows a broad customer base to get a fuel economy benefit. This vehicle participated in the Bibendum Challenge of Paris 2006 and has performed different road driving tests with data recording in Aachen, as well as cranking tests in the lab.

4.2. Test of HEV 6 V modules in micro- and mild hybrid vehicles

Siemens VDO (DE) has adapted a mild hybrid VW Golf IV (Fig. 11c) with a 1.6 L gasoline engine, a 4 kW integrated starter generator and automated manual transmission (AMT), and installed a 48 V/24 Ah battery inside the vehicle trunk. The vehicle includes the following functions; stop-start automatic, warm and cold start, electric boost and launch assist and regenerative braking. Main control strategies (regenerative braking and engine stop request), have been updated, to adapt them to the battery characteristics. The road tests are performed on a special driving cycle, with urban and suburban parts, inside the city of Regensburg, monitoring battery data and cycle data (number of stop-start situations, recuperated energy, fuel consumption,. . .). For the bench tests two different driving cycles: the New European Driving Cycle (NEDC) and the HYZEM City Cycle (HYZEM urban part) will be used.

Ford (DE) plans also to test a 36 V 24 Ah battery in a Transit microhybrid delivery van (HYTRANS project, Fig. 11d), a 2.0 L diesel commercial vehicle with five-speed manual transmission and 42 V belt driven integrated starter generator state-of-the-art components for stop-start operation, regenerative braking and stall protection. It shows a fuel economy benefit on NEDC homologation cycle of 5–6%, although it can reach up to 21% in real use, depending on traffic conditions.

Results of these in-vehicle tests, as well as the study of the ageing effects in the vehicle in comparison to batteries tested in benches in the laboratory, will be reported separately.

5. Conclusions

Former work on the optimisation of spiral wound VRLA battery design and components, including active material formulations, for battery operation under partial-state-of-charge working conditions, has led to the final development of two battery sizes to meet the requirements of automotive manufacturers for micro- and mild hybrid vehicles:

- A 12 V 50 Ah battery for conventional vehicles with stop-start function and microhybrid vehicles with stop-start and regenerative braking (14 V powernet).
- 6 V 24 Ah modules for mild hybrid vehicles with higher powernet voltage, and including stop-start, regenerative braking and boosting functions.

The power capability characterisation at 25 °C showed that the batteries can provide up to 380–420 W kg^{-1} as 10 s average discharge power at 100% SoC, i.e. 2 kW each 6 V 24 Ah module and 7 kW the 12 V 50 Ah battery.

A cycle life test has been defined to test the batteries simulating stop-start operation, at 80% SoC and 2% DoD. The life test has not been completed yet, although results obtained up

to date show a clear improvement of the spiral wound VRLA batteries specifically developed for hybrid vehicle (HEV) operation, when compared to SLI designs. SLI batteries failed after 80,000–90,000 cycles, whereas after 100,000 cycles, HEV prototypes retain over 80% of the initial capacity and have only lost 15–20% of the initial power capability.

In the shallow cycle life test under moderate rate and partial-state-of-charge conditions, the spiral wound modules for HEV completed over 60 life units, which represents more than three times the performance requested by some car manufacturers to prismatic AGM batteries (18 life units) and ten times that requested to flooded SLI batteries (6 life units).

Test of modules with two types of graphite compounds showing similar physical characteristics (BET and average particle size) led to different results in the power assist cycle life test, both in terms of duration and capacity along the test. Test results showed that the best performance was obtained with modules including expanded graphite in the negative active material formulation. These modules completed 220,000 power assist cycles at 60% SoC and 2.5% DoD, which is equivalent to 5,500 capacity turnovers. This result supports the high potential of spiral wound VRLA batteries for short term micro- and mild hybrid applications, due to their availability, cost and improved cycling performance.

Acknowledgements

This work has been partially funded by the Advanced Lead Acid Battery Consortium. The collaboration of PSA, Ford FFA, Valeo, Siemens VDO Automotive and Besel for the in-vehicle test of the batteries in real working conditions is fully acknowledged.

References

[1] E. Karden, S. Ploumen, B. Fricke, T. Miller, K. Snyder, J. Power Sources 168 (2007) 2–11.
[2] M. Anderman, J. Power Sources 127 (2004) 2–7.
[3] Well-to-Wheels Analysis of future automotive fuels and powertrains in the European context), EUCAR Report, November 2003.
[4] E. Karden, P. Shinn, P. Bostock, J. Cunningham, E. Schoultz, D. Kok, J. Power Sources 144 (2005) 505–512.
[5] N. Sato, Proceedings of the Third International Advanced Automotive Battery Conference, Nice, June 2003, Session 3A.
[6] P. Reasbeck, J.G. Smith, Batteries for Automotive Use, Research Studies Press Ltd., Baldock, Hertfordshire, England, 1997.
[7] D. Berndt, J. Power Sources 100 (2001) 29–46.
[8] P. Ruetschi, J. Power Sources 127 (2004) 33–44.
[9] P.T. Moseley, D.A.J. Rand, J. Power Sources 133 (2004) 104–109.
[10] S. Fouache, A. Chabrol, G. Fossati, M. Bassini, M.J. Sáinz, L. Atkins, J. Power Sources 78 (1999) 12–22.
[11] S. Fouache, J.P. Douady, G. Fossati, C. Pascon, J. Power Sources 67 (1997) 15–26.
[12] F. Trinidad, F. Sáez, J. Valenciano, J. Power Sources 95 (2001) 24–37.
[13] R.D. Brost, in: D.A.J. Rand, P.T. Moseley, J. Garche, C.D. Parker (Eds.), Valve Regulated Lead-acid Batteries, Elsevier, Amsterdam, 2004, pp. 327–396.
[14] F. Trinidad, C. Gimeno, J. Gutiérrez, R. Ruiz, J. Sáinz, J. Valenciano, J. Power Sources 116 (2003) 128–140.
[15] J. Valenciano, A. Sánchez, F. Trinidad, A.F. Hollenkamp, J. Power Sources 158 (2006) 851–863.
[16] M.L. Soria, F. Trinidad, J.M. Lacadena, A. Sánchez, J. Valenciano, J. Power Sources 168 (2007) 12–21.
[17] EUCAR Traction Battery Working Group: specification of test procedures for hybrid electric vehicle traction batteries, September 1998.
[18] M.L. Soria, J.C. Hernández, J. Valenciano, A. Sánchez, F. Trinidad, J. Power Sources 144 (2005) 473–485.
[19] L.T. Lam, N.P. Haigh, C.G. Phyland, A.J. Urban, J. Power Sources 133 (2004) 126–134.
[20] Advanced Lead Acid Battery Consortium, Demonstration Project DP1.2, 2006.